

PSD: Parallel Finite Element Solver for Continuum Dynamics

Mohd Afeef Badri  , Giuseppe Rastiello  , and Evelyne Foerster  

1 Université Paris-Saclay, CEA, Service de Génie Logiciel pour la Simulation (SGLS), 91191,
2 Gif-sur-Yvette, France 2 Université Paris-Saclay, CEA, Service d'Études Mécaniques et Thermiques
3 (SEMT), 91191, Gif-sur-Yvette, France 3 Université Paris-Saclay, CEA, Département de Modélisation
des Systèmes et Structures (DM2S), 91191, Gif-sur-Yvette, France ¶ Corresponding author

DOI: [10.xxxxxx/draft](https://doi.org/10.xxxxxx/draft)

Software

- [Review](#) 
- [Repository](#) 
- [Archive](#) 

Editor: Patrick Diehl  

Reviewers:

- [@nrichart](#)
- [@gtheler](#)

Submitted: 07 October 2025

Published: unpublished

License

Authors of papers retain copyright and release the work under a Creative Commons Attribution 4.0 International License ([CC BY 4.0](#)).


Summary

PSD (Parallel finite element Solver for continuum Dynamics) is an open-source finite element method (FEM) solver designed for high-performance computing simulations in continuum dynamics with a special focus on earthquake mechanics. It enables integrated fault-to-site seismic simulations by combining advanced material modeling, scalable parallelism, and purpose-built meshing-partitioning tools.

Built on FreeFEM ([Hecht, 2012](#)) for FEM discretization and PETSc ([Balay et al., 2019](#)) for scalable linear solvers, PSD integrates non-linear material modeling through its MFront ([Helfer et al., 2015](#)) interface for realistic simulations. Its custom MPI I/O-based mesher–partitioner, top-ii-vol ([Badri et al., 2024](#)), enables efficient on-the-fly mesh generation and partitioning for earthquake geometries, removing sequential meshing bottlenecks. On the structural side, hybrid phase-field fracture mechanics ([Ambati et al., 2015](#)) for crack analysis is implemented. This spans the full simulation chain from earthquake source to structural assessment.

A key feature of PSD is its ability to perform fault-to-site earthquake simulations with billions of degrees of freedom, scaling efficiently on tens of thousands of MPI-processes, making it suitable for comprehensive seismic risk assessment.

Statement of Need

Seismic risk assessment requires tools that can simulate wave propagation across multiple scales, from faults (kilometers away) to local site response (meters), with sufficient accuracy. Commercial software often lacks the scalability needed for regional simulations, while open-source alternatives typically focus on specific parts of the seismic workflow.

Current computational challenges in earthquake simulation include: (1) handling billions of degrees-of-freedom to capture realistic fault-to-site scenarios ([Hori et al., 2018](#)), ([Cui et al., 2013](#)), (2) integrating complex non-linear material behaviors and damage assessment for solids and structures, and (3) efficiently generating and partitioning large meshes for irregular geological domains derived from digital elevation models. FEM tools like OpenSees ([McKenna, 2011](#)) excel in local-site response, while SPECFEM3D ([Peter et al., 2011](#)) and SEM3D ([Touhami et al., 2022](#)) address wave propagation using spectral elements. An open-source platform covering the full fault-to-site workflow with HPC scalability remains highly desirable.

PSD tries to fill this gap by providing a unified framework that combines earthquake wave propagation simulation and structural mechanics assessment within a single scalable FEM solver. PSD's integration of advanced meshing–partitioning capabilities, sophisticated material modeling, and fracture mechanics positions it uniquely for comprehensive seismic risk assessment needs.

⁴¹ requiring both regional-scale wave propagation and local site response, including structural
⁴² analysis.

⁴³ Features and Architecture

⁴⁴ PSD offers a range of physics modules designed for earthquake simulations, including linear
⁴⁵ elasticity, elastodynamics, fracture mechanics, soildynamics ¹, and elasto-plasticity. Its versatility
⁴⁶ is further enhanced by the Mfront interface, which allows users to implement custom non-linear
⁴⁷ material models, that can be seamlessly integrated into any of these modules expanding their
⁴⁸ capabilities beyond its built-in constitutive laws. Additionally, comprehensive verification and
⁴⁹ validation campaigns for all PSD modules, with results cross-compared against reference codes,
⁵⁰ experimental data, and analytical benchmarks, ensuring transparency and reproducibility (see
⁵¹ [validation page](#)).

⁵² PSD adopts a layered architecture that separates mathematical formulation from computational
⁵³ implementation while maintaining high performance through strategic integration. It follows
⁵⁴ a code generation approach where users specify problem configurations through command-
⁵⁵ line options, and the it automatically generates optimized code tailored to specific physics,
⁵⁶ dimensionality, and boundary conditions. This design enables computational efficiency while
⁵⁷ preserving flexibility for diverse applications across the available physics modules.

⁵⁸ The parallel computing architecture in PSD employs domain decomposition strategies that
⁵⁹ enable distributed memory parallelization which are optimized for large-scale FEM simulation
⁶⁰ ([Dolean et al., 2015](#)). PSD has demonstrated scalability up to 24,000 cores and capability for
⁶¹ handling problems with over 5 billion unknowns for earthquakes.

⁶² Example Workflow

⁶³ A representative application illustrates PSD's soildynamics module for 3D wave propagation
⁶⁴ in an elastic domain with paraxial absorbing boundaries ([Modaressi & Benzenati, 1994](#)) and
⁶⁵ double-couple point sources ([Benz & Smith, 1987](#)). This example illustrates one of PSD's
⁶⁶ specialized physics modules, among others. The aim here is to briefly illustrate PSD's key
⁶⁷ capabilities, including automated distributed mesh generation, advanced time integration, and
⁶⁸ sophisticated boundary condition handling.

⁶⁹ **Mathematical Presentation:** PSD solves the elastodynamic wave equation using FEM discretiza-
⁷⁰ tion with Newmark- β time integration. For a domain $\Omega \subset \mathbb{R}^3$ and with paraxial absorbing
⁷¹ boundaries $\partial\Omega_p \subset \partial\Omega$, the FEM weak form reads:

Find $\mathbf{u} \in \mathcal{U}$ such that $\forall t \in [0, t_{\max}], \forall \mathbf{v} \in \mathcal{V}$:

$$\int_{\Omega} \left(\frac{\rho}{\beta \Delta t^2} \mathbf{u} \cdot \mathbf{v} + \boldsymbol{\sigma}(\mathbf{u}) : \boldsymbol{\varepsilon}(\mathbf{v}) \right) + \int_{\partial\Omega_p} \frac{\rho\gamma}{\beta \Delta t} \mathbf{u} \cdot \mathbf{P} \cdot \mathbf{v} = \\ \int_{\Omega} \frac{\rho}{\beta} \left(\frac{1}{\Delta t^2} \mathbf{u}_{\text{old}} \cdot \mathbf{v} + \frac{1}{\Delta t} \dot{\mathbf{u}}_{\text{old}} \cdot \mathbf{v} + \left(\frac{1}{2} - \beta \right) \ddot{\mathbf{u}}_{\text{old}} \cdot \mathbf{v} \right) + \\ \int_{\partial\Omega_p} \left(\frac{\rho\gamma}{\beta \Delta t} \mathbf{u}_{\text{old}} \cdot \mathbf{P} \cdot \mathbf{v} + \left(\frac{\rho\gamma}{\beta} - \rho \right) \dot{\mathbf{u}}_{\text{old}} \cdot \mathbf{P} \cdot \mathbf{v} + \left(\frac{\rho\gamma \Delta t}{2\beta} - \rho \Delta t \right) \ddot{\mathbf{u}}_{\text{old}} \cdot \mathbf{P} \cdot \mathbf{v} \right).$$

⁷² Here, (\mathbf{u}, \mathbf{v}) are the FEM trial and test functions, respectively, defined in FEM linear closed
⁷³ space. $(\mathcal{U}, \mathcal{V})$ defined in $[H^1(\Omega)]^3$, for further details see PSD's soildynamics [documentation](#).

¹The *soildynamics* module builds upon the *elastodynamics* module by adding tools essential for earthquake modeling, such as paraxial boundary conditions, double-couple source mechanisms, point-cloud meshing-partitioning, etc.

74 **Execution Workflow:** PSD begins with automated code generation through the PSD_PreProcess
 75 utility, which generates problem-specific FEM code based on user specifications.

76 PSD_PreProcess -problem soildynamics -dimension 3 -top2vol-meshing \
 77 -timediscretization newmark_beta -postprocess uav

78 Typical soil properties and time-integration parameters are included:

```
79       real rho = 1800.0 , // Density
80       cs = 2300.0 , // S-wave velocity
81       cp = 4000.0 ; // P-wave velocity
82
83       real tmax = 20.0 , // Total time
84       t = 0.001 , // Initial time
85       dt = 0.001 ; // Time step
```

86 The simulation is executed using the parallel solver with the specified number of MPI-processes:

87 PSD_Solve -np 6144 Main.edp

88 Results such as those presented in Figure 1 can be obtained.

89 **Demonstration**

90 Figure 1 presents a regional-scale earthquake simulation of the Cadarache region in France (50
 91 km × 50 km) performed with PSD (Badri et al., 2024), comprising over one billion degrees
 92 of freedom distributed across 6144 MPI-domains on a 540-million-element mesh with 10 m
 93 resolution.

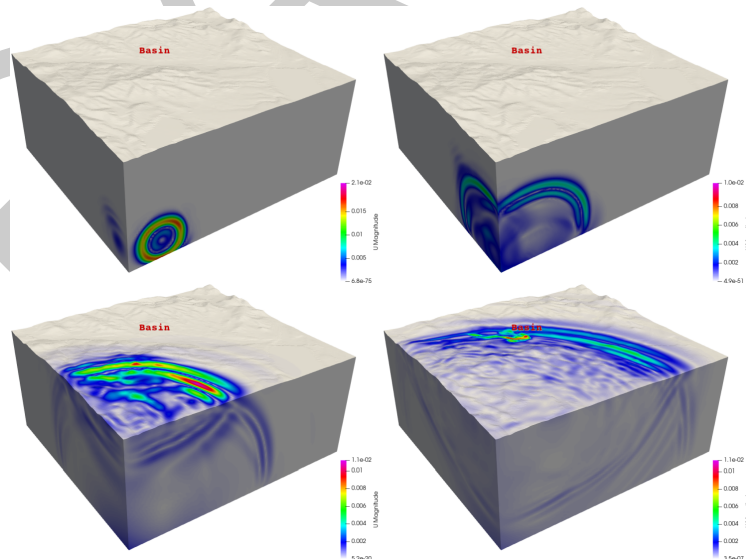


Figure 1: Earthquake simulation of the French Cadarache region showing displacement magnitude at four time steps.

94 Figure 2 demonstrates fracture mechanics capabilities through quasi-static brittle fracture
 95 simulation in a perforated medium (Badri et al., 2021), involving more than 64 million degrees
 96 of freedom across 1008 MPI-domains, illustrating detailed damage assessment capabilities.

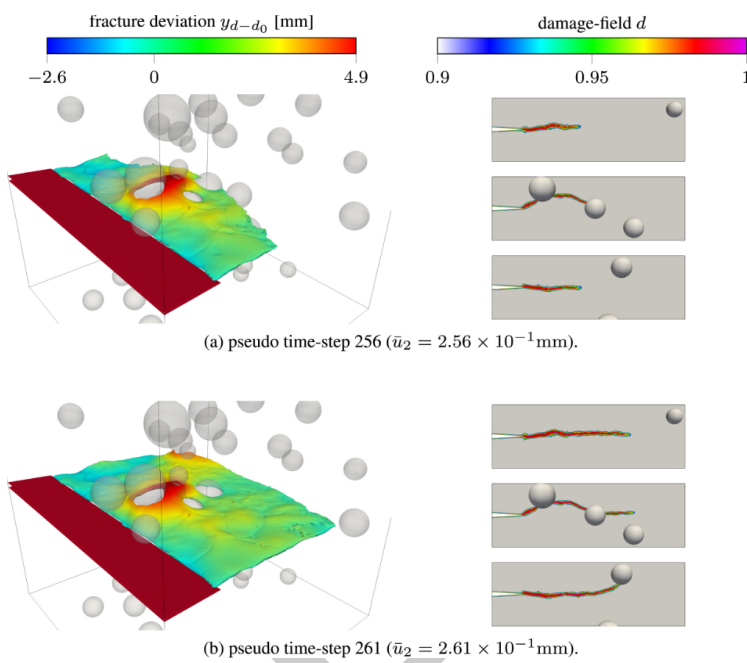


Figure 2: Crack propagation for a perforated medium.

These demonstrations represent significant computational achievements, with problem sizes approaching those required for seismic hazard and risk assessment. The Cadarache region simulation underscores PSD's applicability to real-world earthquake engineering, while the fracture mechanics case illustrates its capability for detailed damage analysis. Further applications, including eikonal non-local gradient damage models (Nogueira et al., 2023), (Nogueira et al., 2024), highlight PSD's versatility and its potential for comprehensive structural and fracture mechanics research.

104 Acknowledgements

105 This work is supported by the French Alternative Energies and Atomic Energy Commission
 106 (CEA) through the GEN2&3 program. G. Rastiello was also supported by the SEISM Institute
 107 (France). The authors thank Dr. Breno Ribeiro Nogueira for advanced fracture module,
 108 Dr. Reine Fares for nonlinear soil modeling, and Rania Saadi for the parallel mesh adaptation
 109 kernel.

110 References

- 111 Ambati, M., Gerasimov, T., & De Lorenzis, L. (2015). A review on phase-field models of
 112 brittle fracture and a new fast hybrid formulation. *Computational Mechanics*, 55, 383–405.
 113 <https://doi.org/10.1007/s00466-014-1109-y>
- 114 Badri, M. A., Bourcier, C., & Foerster, E. (2024). Top-ii-vol: Massively parallel scalable
 115 meshing for seismic risk assessment of nuclear sites. *EPJ Web of Conferences*, 302, 05007.
 116 <https://doi.org/10.1051/epjconf/202430205007>
- 117 Badri, M. A., Rastiello, G., & Foerster, E. (2021). Preconditioning strategies for vectorial finite
 118 element linear systems arising from phase-field models for fracture mechanics. *Computer
 119 Methods in Applied Mechanics and Engineering*, 373, 113472. <https://doi.org/10.1016/j.cma.2020.113472>

- 121 Balay, S., Abhyankar, S., Adams, M., Brown, J., Brune, P., Buschelman, K., Dalcin, L.,
 122 Dener, A., Eijkhout, V., Gropp, W., & others. (2019). *PETSc users manual*. <https://doi.org/10.2172/1814627>
- 124 Benz, H. M., & Smith, R. B. (1987). Kinematic source modelling of normal-faulting earthquakes
 125 using the finite element method. *Geophysical Journal International*, 90(2), 305–325.
 126 <https://doi.org/10.1111/j.1365-246x.1987.tb00729.x>
- 127 Cui, Y., Poyraz, E., Olsen, K. B., Zhou, J., Withers, K., Callaghan, S., Larkin, J., Guest,
 128 C., Choi, D., Chourasia, A., & others. (2013). Physics-based seismic hazard analysis on
 129 petascale heterogeneous supercomputers. *Proceedings of the International Conference on*
 130 *High Performance Computing, Networking, Storage and Analysis*, 1–12. <https://doi.org/10.1145/2503210.2503300>
- 132 Dolean, V., Jolivet, P., & Nataf, F. (2015). *An introduction to domain decomposition
 133 methods: Algorithms, theory, and parallel implementation*. SIAM. <https://doi.org/10.1137/1.9781611974065>
- 135 Hecht, F. (2012). New development in FreeFem++. *Journal of Numerical Mathematics*,
 136 20(3-4), 251–265. <https://doi.org/10.1515/jnum-2012-0013>
- 137 Helfer, T., Michel, B., Proix, J.-M., Salvo, M., Sercombe, J., & Casella, M. (2015). Introducing
 138 the open-source mfront code generator: Application to mechanical behaviours and material
 139 knowledge management within the PLEIADES fuel element modelling platform. *Computers
 140 & Mathematics with Applications*, 70(5), 994–1023. <https://doi.org/10.1016/j.camwa.2015.06.027>
- 142 Hori, M., Ichimura, T., Wijerathne, L., Ohtani, H., Chen, J., Fujita, K., & Motoyama, H. (2018).
 143 Application of high performance computing to earthquake hazard and disaster estimation in
 144 urban area. *Frontiers in Built Environment*, 4, 1. <https://doi.org/10.3389/fbuil.2018.00001>
- 145 McKenna, F. (2011). OpenSees: A framework for earthquake engineering simulation. *Computing
 146 in Science & Engineering*, 13(4), 58–66. <https://doi.org/10.1109/MCSE.2011.66>
- 147 Modaressi, H., & Benzenati, I. (1994). Paraxial approximation for poroelastic
 148 media. *Soil Dynamics and Earthquake Engineering*, 13(2), 117–129. [https://doi.org/10.1016/0267-7261\(94\)90004-3](https://doi.org/10.1016/0267-7261(94)90004-3)
- 150 Nogueira, B. R., Rastiello, G., Giry, C., Gatuingt, F., & Callari, C. (2024). Eikonal gradient-
 151 enhanced regularization of anisotropic second-order tensorial continuum damage models
 152 for quasi-brittle materials. *Computer Methods in Applied Mechanics and Engineering*, 429,
 153 117100. <https://doi.org/10.1016/j.cma.2024.117100>
- 154 Noigueira, R. B., Rastiello, G., Giry, C., Gatuingt, F., & Callari, C. (2023). Numerical
 155 simulations of concrete specimens with the gradient-enhanced Eikonal non-local damage
 156 model. *Academic Journal of Civil Engineering*, 41(1). <https://doi.org/10.26168/ajce.41.1.30>
- 158 Peter, D., Komatitsch, D., Luo, Y., Martin, R., Le Goff, N., Casarotti, E., Le Loher, P.,
 159 Magnoni, F., Liu, Q., Blitz, C., Nissen-Meyer, T., Basini, P., & Tromp, J. (2011). Forward
 160 and adjoint simulations of seismic wave propagation on fully unstructured hexahedral
 161 meshes. *Geophysical Journal International*, 186(2), 721–739. <https://doi.org/10.1111/j.1365-246X.2011.05044.x>
- 163 Touhami, S., Gatti, F., Lopez-Caballero, F., Cottereau, R., Abreu Corrêa, L. de, Aubry, L.,
 164 & Clouteau, D. (2022). SEM3D: A 3D high-fidelity numerical earthquake simulator for
 165 broadband (0–10 hz) seismic response prediction at a regional scale. *Geosciences*, 12(3),
 166 112. <https://doi.org/10.3390/geosciences12030112>